

Polyaniline-modified graphene oxide nanocomposites in epoxy coatings for enhancing the anticorrosion and antifouling properties

Sara Fazli-Shokouhi, Farzad Nasirpouri, Maasoumeh Khatamian

© American Coatings Association 2019

Abstract We report on the anticorrosion and antifouling properties of epoxy-based polyaniline (PANI)–graphene oxide nanosheets (GONs) paint coatings. PANI-based nanocomposites with different fractions of GONs were synthesized by an in situ polymerization process. Well-dispersed GONs were prepared using a modified Hummers' method in the presence of $(\text{NH}_4)_2\text{S}_2\text{O}_8$ as an effective oxidant. We employed a spontaneous in situ polymerization at a constant temperature of 0°C using an ultrasonic bath to produce homogenous PANI-GON nanocomposites as characterized by X-ray diffraction (XRD), Fourier transfer infrared spectroscopy (FTIR), and field-emission scanning electron microscopy (FESEM) techniques. The nanocomposites were incorporated into an epoxy resin with different fractions to form epoxy/PANI-GON paint coatings. The epoxy/PANI-GON dip coated on a carbon steel (grade St-37) substrate exhibited significant improvement of the anticorrosion and antifouling properties. Epoxy-12 wt% PANI-GON coating revealed the highest corrosion resistance of $2.70 \times 10^6 \Omega \text{ cm}^2$ after 192-h immersion in saline water measured by electrochemical impedance spectroscopy (EIS) technique. Such high corrosion resistance was attainable by inhibiting the diffusion process against the corrosive environment. Furthermore, higher protection against fouling was observed for epoxy 6 and 12 wt% PANI/GON as the most efficient antifouling composite coatings.

Keywords Graphene oxide nanosheet (GON), Polyaniline (PANI), Epoxy, Anticorrosion, Antifouling

Introduction

Corrosion and its prevention impose remarkable costs to modern and industrial societies.^{1,2} One of the widespread methods for corrosion protection is to apply coatings on the surface of metals and alloys.³ Nanoparticles have been significantly used for producing functional nanocoatings with anticorrosion, waterproof, antistick, antifog and antifouling properties. The methods of application of nanocoatings onto the surfaces are vast and may be classified into chemical precipitation, physical precipitation, electrochemical deposition, sol–gel, laser method, and other techniques.^{4,5}

Biofouling is one of the serious problems in marine applications which causes air pollution and water contamination.^{6,7} Different factors like temperature, salinity, nutrients, flow rate, and intensity of sunlight irradiation control the fouling growth.^{8–10} Over the recent decades, antifouling coatings have been applied to surfaces by using tributyltin, tributyltin oxides or some metal oxides. This kind of biocide coating has widespread use in the field of sailing and may restrict fouling growth on the surface for about 5 years. Scientists gradually noticed the negative influence of this kind of material on animals and human beings. Hence, governments were about to prohibit their use. New methods for preventing fouling growth have been therefore designed such as novel functional coatings which are safer to the environment.^{6,7}

Graphene is one of the effective materials with higher anticorrosion properties when introduced as a filling constituent into polymer matrices.^{3,11} It has one-atom-thick sheets of covalently bonded carbon

S. Fazli-Shokouhi, F. Nasirpouri (✉)
Faculty of Materials Engineering, Sahand University of
Technology, Tabriz, Iran
e-mail: nasirpouri@sut.ac.ir; f_nasirpouri@yahoo.com

M. Khatamian
Department of Inorganic Chemistry, Faculty of Chemistry,
University of Tabriz, Tabriz, Iran

atoms, shaped in a honeycomb crystal lattice which exhibit remarkable mechanical, thermal conductivity, and electronic transport properties making it a revolutionary material for the 21st Century.¹² Graphene oxide (GO) is one of the important graphene derivatives, which can be produced by attaching some oxygen functional groups (e.g. hydroxyl, carboxyl, and epoxide group) to the base of the planes or edges of graphene sheets. The contribution of oxygen functional groups are inhomogeneous, providing high specific surface area, delocalizing negative charge of surface, and improving hydrogen bonding, which facilitate the formation of composites with other materials.^{13–15} GO has been widely used in solar cells, supercapacitors, biosensors, gas sensors, and functional coatings.^{16–19}

Epoxy and its nanocomposites have widespread usages worldwide in aerospace, maritime, sport equipment, buildings, electronic systems, bio-medicine, and in production of anticorrosion coatings.²⁰ This kind of coating has poor quality because of its high porosity, which leads to the penetration of corrosive elements.²¹ Scientists and researchers in different fields are interested in studying new ways and in finding effective additive materials to improve the quality of epoxy coatings. Three major methods include: (1) reinforcement of the epoxy with conductive polymers, (2) reinforcement of the epoxy coating with inorganic materials, in pure form or connected by hybridization with graphene oxide, and (3) reinforcement of the epoxy coatings with conductive composites of polymer nanoparticles or composites of conductive polymer-graphene derivatives.

It is noteworthy that conductive polymers have some good effects on the suppression of corrosion. First, they change the oxidation potential which results in the corrosion prevention and protection of the metal in a passive form.^{22,23} Second, they change the electrochemical interface properties by creating more distance from the surface.²⁴ On the other hand, inorganic materials can be considered as the second phase in the epoxy matrix.²⁵ They have the ability to fill the micropores in the epoxy coating. Dispersion of the inorganic nanoparticles in the structure of the epoxy will create zigzag-shaped paths for diffusion of the corrosive elements.^{26–31} The cooperative effect of the nanoparticles and conductive materials will improve the anticorrosive properties. There has been successful research from our group on the influence of PANI-ZnO on improving antifouling and anticorrosion properties of epoxy-based paint coatings.^{32–34} Although using the composites of conductive polymers with graphene derivatives to improve the quality of coatings is an interesting challenge, few papers are published on the subject. Jafari et al. investigated the corrosion protection properties of the polyaniline-graphene nanocomposite films co-electrodeposited on 310 stainless steel substrate. It was reported that the coating resistance could not raise more than 13 k Ω in the 3.5% NaCl aqueous solution.³⁵ A. Mooss et al.

studied the anticorrosion property of the graphene oxide-modified polyaniline pigment of epoxy. This coating which they called PG1-painted, showed a 14.81 k Ω resistance on low carbon steel after 96 h immersion. They used different materials such as titanium dioxide and di-octyl phthalate to improve the viscosity and elastic properties of the paint.³⁶

The main idea of this study was to produce graphene oxide nanosheets (GONs) to be added to PANI, making PANI-GON nanocomposites as an effective pigment for epoxy binder. The goal product, epoxy-based PANI-GON nanocomposite paint coatings, was investigated to exploit its anticorrosion properties. The other main objective of the study was to introduce an environmentally friendly marine paint which can suppress or prevent fouling processes on the manufactured surfaces immersed in sea water. An appropriate corrosion protection and antifouling mechanism of iron in the presence of epoxy-based PANI-GON nanocomposite coatings is proposed.

Experimental

Materials and instruments

Natural graphite and sulfuric acid (H₂SO₄, 98%) were obtained from Merck 100713, sodium nitrate (NaNO₃) from Merck 6535, potassium permanganate (KMnO₄) from Merck 105080, hydrochloric acid (HCl, 35.4%) from Royalex-H125, hydrogen peroxide (H₂O₂, 35%) from Merck, ethanol (C₂H₅OH 99.5%), aniline from Merck 822256, ammonium persulfate (APS) from Merck-1.01209, NAYA epoxy resin (NPEL-127), ACR hardener (H3895), NaCl from Fluka AG-218541280, deionized water.

A Bruker Tensor 27 Fourier transform infrared spectrometer (FTIR) utilizing KBr pellet method was used. Field-emission scanning electron microscopy (FESEM) images were taken by a MIRA TESCAN scanning electron microscope operating at 15 kV. The X-ray diffraction (XRD) patterns of powder nanocomposite were obtained by a Bruker D8 Advance AXS diffraction utilizing Cu K α radiation source ($\lambda = 1.54 \text{ \AA}$) performed at 40 kV and 40 mA in the 2θ ranging 10°–80° with a scan rate of 0.05° per second. Electrochemical measurements for the corrosion protection were investigated in a three-electrode conventional test cell controlled by an Autolab PG STAT 30 instrument in the 3.5% NaCl solution. The exposed area of coating test specimens for studying the corrosion behavior was 1.00 cm². A standard Ag/AgCl electrode and a platinum electrode were taken as the reference electrode and the counter electrode, respectively. All the electrochemical examinations were done in a conventional three-electrode cell including the coated steel as the working electrode, a Pt electrode as the counter electrode and Ag/AgCl electrode in an electrolyte of 3.5% NaCl solution. Electrochemical

impedance spectroscopy (EIS) tests were obtained by applying a perturbation voltage of 5 mV (rms) in a frequency range of 10 kHz to 100 mHz. The Nyquist and bode plots, which were obtained by EIS tests, were numerically fitted using ZView® (II) software to determine the equivalent electrical circuit parameters. Finally, thickness of the paint coatings was measured by an eXacto FN elcometer.

Synthesis of graphene oxide

Graphene oxide nanosheets (GON) were prepared by a modified Hummers' method according to references (37) and (38): 2.0 g of graphite powder and 1.0 g of NaNO₃ were put into a 500-mL round-bottom flask. Then 62 mL of H₂SO₄ was added. The mixture was prepared in an ice bath for 1 h. (Temperature was adjusted to maintain under 20°C.) Next, 6 g of KMnO₄ as an oxidizing agent was added in 30 min (1 g per 5 min) and 2 g of (NH₄)₂S₂O₈ agent as a promoter of oxidation process was added stepwise in 50 min (in each step 0.2 g every 5 min). These were estimated to be added very slowly to the mentioned flask. The reaction took place under reflux conditions for 24 h. Subsequently, 140 mL of deionized water was added to the mixture in a dropwise manner. Afterward, the mixture's temperature was increased to 80°C. At this stage, tiny golden particles were seen in the mixture. Later, 34 mL of H₂O₂ (32.4%) was added. For removing the salt ions, 22.6 mL HCl (35.4%) was added to the mixture. After 10 min, 80 mL deionized water was slowly added to the mixture. The mixture was then centrifuged and washed several times until the pH reached 7.

Synthesis of PANI-GON nanocomposites

For preparation of GON/PANI nanocomposites, first, a certain amount of GON was dispersed into 25 mL of deionized water in an ultrasonic bath for 1 h. Then, the GON suspension was added into 2 mL of aniline, dissolved before in 100 mL 1 M HCl (35.4 vol%). After stirring in an ice bath for 30 min, the mixture was sonicated under 305 W, 50/60 Hz for 1 h to disperse aniline monomers homogeneously with GONs. Next, 100 mL of 1 M HCl solution containing 4.8 g (NH₄)₂S₂O₈ was added dropwise at a rate of 0.5 mL per min into the mixture in an ice-water bath under magnetic stirring with a nominal rotation speed of 700 rpm. The in situ polymerization was conducted at 0°C for 3 h. Afterward, the mixture was sonicated for 2 h in order to avoid the aggregation of polymeric constituent. The products were filtered and repeatedly washed with ethanol and deionized water several times until the filtrate solution became colorless. The synthesized composites were dried under vacuum at 60°C for 5 h.^{39,40} The synthesis procedure for PANI-GON is schematically illustrated in Fig. 1.

Preparation of the PANI-GON composite coatings

Carbon steel grade st-37 substrates with 1 cm × 1 cm dimensions were mechanically polished by grinding sand paper with meshes razing 80 up to 2000. Then, they were rinsed with deionized water in the beaker in ultrasonic bath for 2 min and dried. The epoxy emulsion was mixed with 2 wt% PANI-GON composites under magnetic stirring with a nominal speed of 300 rpm for 30 min. Then, the coating materials were sonicated for 45 min. Sonication not only facilitates the dispersion of nanocomposites within the epoxy emulsion but also removes the bubbles, which were produced during magnetic stirring. In the following, the hardener was poured into the epoxy mixture with 1:2 weight ratio (1: hardener, 2: epoxy) and mixed very slowly. The polymer epoxy paints with different percentages of nanocomposites were applied onto the steel substrate by dip-coating method to create a smooth and homogenous film on the substrates until the epoxy started to become viscous. Then, the coating was dried at room temperature for 24 h. The thickness of the coatings produced was around 200 ± 15 μm which is consistent with general marine coating specifications.

Antifouling properties of epoxy-based PANI-GON nanocomposite coatings

Antifouling test specimens were prepared by cutting carbon steel grade st-37 plates in 3 × 4 cm² disks and dip coated with the epoxy-based PANI/GON paint according to the procedure described in "Preparation of the PANI-GON composite coatings" section. In order to control different parameters for simulated fouling conditions and environment, we set up an antifouling test chamber equipped with oxygen pump, thermometer, LED lamp, and heater. The temperature was kept constant in a range of 25–27°C which is a suitable level for fish and plant growth, spirulina algae, guppy fish and dwarf hair grass.

Results and discussion

FTIR study

FTIR spectra of GON are shown in Fig. 2. We find that oxidizing process of graphite was successful when we used (NH₄)₂S₂O₈ as an additive. Two types of (–OH) groups were detected: hydroxylic OH and phenolic OH. The phenolic OH facilitates the dispersion of the graphene sheets in deionized water. This will in turn have a positive effect on the preparation of different fractions of GON in PANI composites.

The FTIR spectrum clearly shows a broad peak in a range of 3000–3500 cm^{–1} which corresponds to –OH stretching vibration.⁴¹ The peak occurring at 1745 cm^{–1}

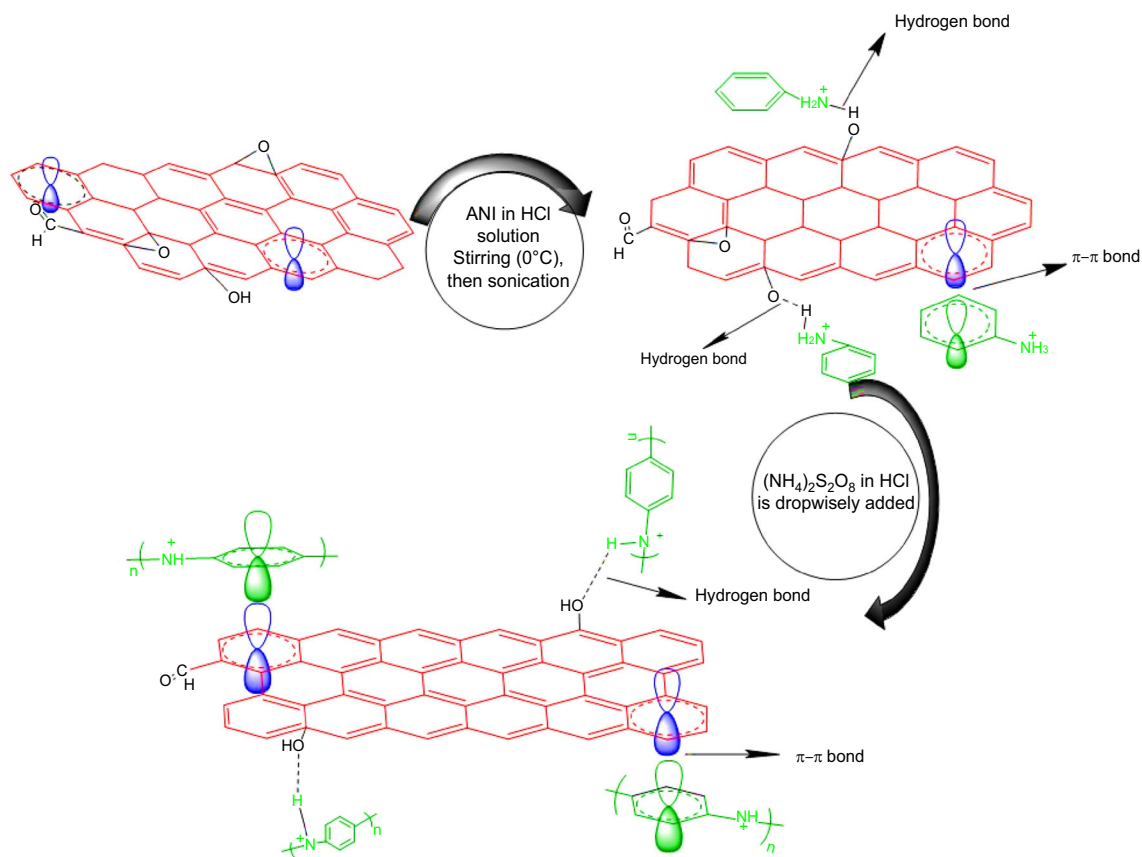


Fig. 1: Illustration of the synthesis procedure for PANI-GON

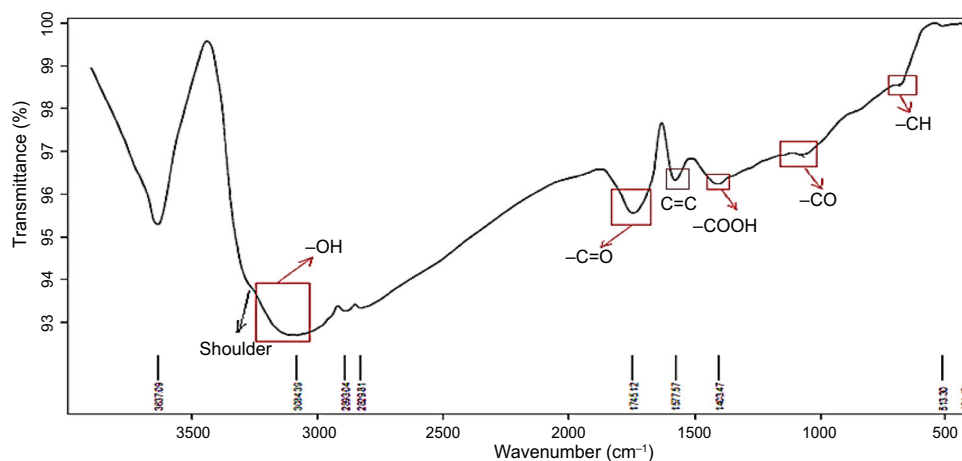


Fig. 2: FTIR spectra of synthesized GON from modified Hummers' method by adding more oxidant $[(\text{NH}_4)_2\text{S}_2\text{O}_8]$

is attributed to $(-\text{C}=\text{O}-)$ stretching vibration. The peaks seen at 1577, 1403.75, and 1075 cm^{-1} represent C=C, C-OOH, and C-O vibrations, respectively.^{42,43} The wide adsorption peak at 690 cm^{-1} is related to the C-H bonding.⁴³ Shunaev and Glukhova studied important factors for oxidizing the graphene sheets.⁴⁴ Based on theoretical assumptions and experimental data,⁴⁴ it has been concluded that the amount of activation

barrier energy for epoxy groups is higher than that for hydroxyl groups. Furthermore, if the number of the graphene sheets increases, the activation energy for oxidizing will decrease facilitating the oxidation process of graphite. Hence, the FTIR spectrum of prepared GONs from graphite exhibits an intense and broad peak for $(-\text{OH})$ groups due to the large number of these groups.

FTIR spectra of PANI, GON, PANI-3 wt% GON-, PANI-6 wt% GON, PANI-12 wt% GON, and PANI-24 wt% GON are shown in Fig. 3. In Fig. 3a, FTIR spectrum of polyaniline always elucidates the adsorption peaks at 1106, 1294, 1480, and 1563 cm^{-1} .³⁷ Strong adsorption peaks at 1480 cm^{-1} and 1563 cm^{-1} show the benzene ring and the quinone ring, respectively. Adsorption peak of benzene ring is stronger than that of quinone ring indicating that the synthesized polyaniline has the emeraldine form.⁴¹ The adsorption peaks at 1127 and 795 cm^{-1} represent stretching vibration inside and outside of the C-H molecular plane. 1294.47 cm^{-1} and 1241 cm^{-1} peaks correspond to stretching vibration of $-\text{C}-\text{N}$ and $-\text{C}=\text{N}$, respectively.⁴² Focusing on the FTIR of PANI and PANI/GON nanocomposites with different GON fractions, it can be noticed that the peak at 1563 cm^{-1} in FTIR spectrum of PANI has a blueshift detected at higher wavenumbers. By increasing the fraction of GON in the structure of nanocomposites, the peaks related to OH, CO, COOH bonds appear. The connection between PANI chains and GONs can be related to three types of energy factors including the electrostatic energy, the hydrogen bonding and $\pi-\pi$ stacking. The oxygen groups like OH, COOH, CHO, and epoxy on the graphene sheets can make the surface of the sheets more electronegative than before. PANI would be protonated by oxidation reaction, which is facilitated

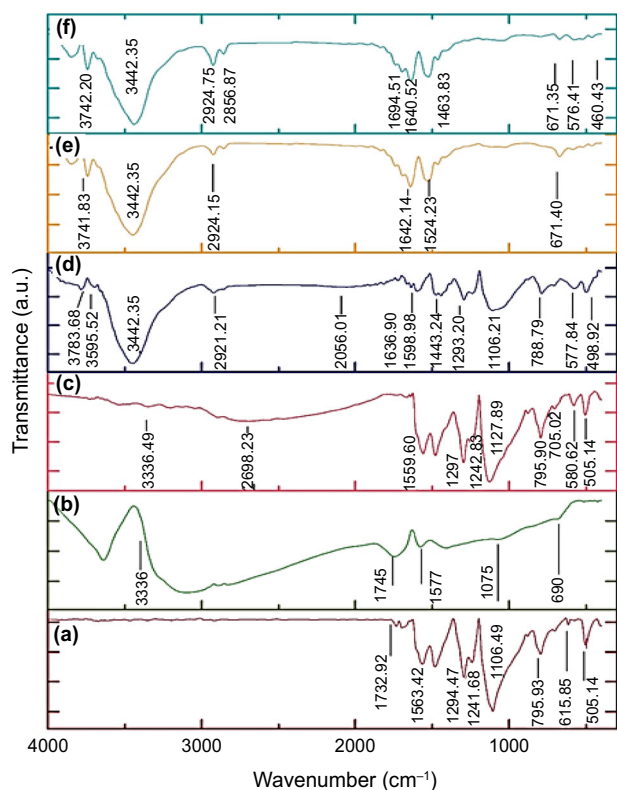


Fig. 3: FTIR spectrum of (a) polyaniline, (b) GON, (c) PANI-GON (3 wt%), (d) PANI-GON (6 wt%), (e) PANI-GON (12 wt%), and (f) PANI-GON (24 wt%)

by HCl, and it would have electropositive property. In this way, the electrostatic attraction between GON and PANI has been reinforced. Moreover, the graphene oxides play the templating role, which helps nucleation of polyaniline.^{40,45,46} The FTIR spectra of GON, PANI-GON (3 wt%), PANI-GON (6 wt%), PANI-GON (12 wt%), and PANI-GON (24 wt%) are shown in Figs. 3b, 3c, 3d, 3e, and 3f, respectively.

XRD analysis

The XRD pattern of GONs prepared using Hummer's method is shown in Fig. 4. The characteristic Bragg diffraction of graphene oxide occurs at $2\theta = 11.57^\circ$ which is observed after oxidizing the graphite flakes. The characteristic Bragg diffraction peak of graphite ($2\theta = 26.5^\circ$) was omitted. After using Hummer's method for oxidation of the graphite flake, the interplanar distance between flakes increases from 0.35 to 0.77 nm for graphene oxide. This increase was estimated by using the Bragg equation, equation (1).⁴⁷ The mentioned increment of the distance between the graphene sheets can be due to the presence of functional groups $-\text{OH}$, $\text{C}=\text{O}$, $\text{C}-\text{O}$, and $\text{C}-\text{OOH}$ in graphene oxide structure.

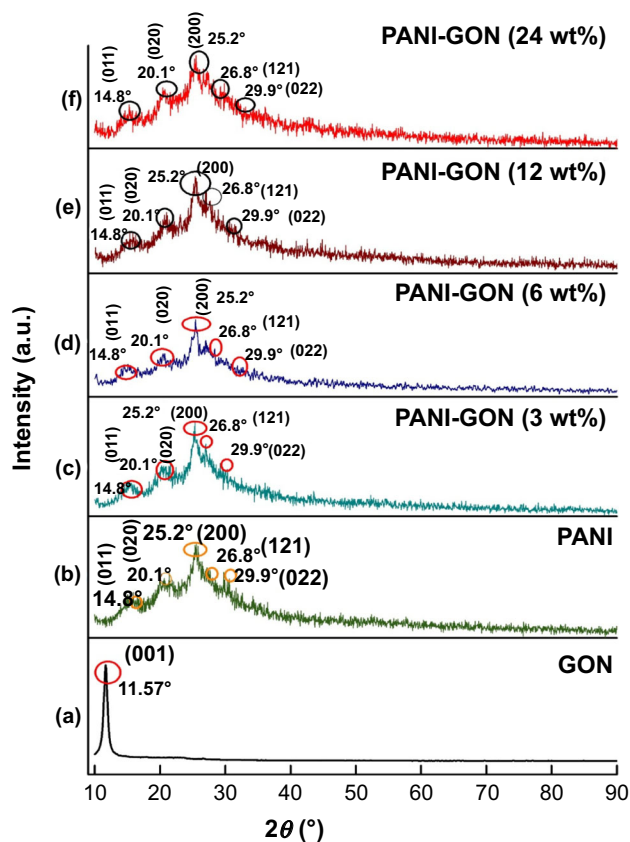


Fig. 4: XRD patterns of (a) GON, (b) PANI, (c) PANI-GON (3 wt%), (d) PANI-GON (6 wt%), (e) PANI-GON (12 wt%), (f) PANI-GON (24 wt%)

$$2d \cdot \sin \theta = n\lambda, \quad (1)$$

where $\lambda = 1.54 \text{ \AA}$, $n = 1$.

We have also examined the crystalline structure of PANI/GON nanocomposites by XRD. Polyaniline was synthesized in HCl medium. HCl may likely improve the orientation of polyaniline structure, resulting in enhanced crystallinity. This polymer has characteristic peaks at 9.5° , 14.8° , 20.1° , 25.2° , 26.8° , and 29.9° , corresponding to (001), (011), (020), (200), (121), and (022) planes of emeraldine form crystals of polyaniline, respectively, as shown in Fig. 4b.⁴⁰ The XRD patterns of synthesized PANI/GON nanocomposites with different percentages of GON are shown in Figs. 4c, 4d, 4e, and 4f. As can be seen, the characteristic peak of GO ($2\theta = 11.4^\circ$) of the mentioned composites has disappeared. The XRD patterns of synthesized PANI/GON nanocomposites are the same as that of PANI.⁴⁶ Thus, it can be deduced that GONs are completely exfoliated, and polyaniline chains are formed between GO sheets.⁴⁸ The XRD patterns with the different percentages of GON confirm the simultaneous presence of both GO and PANI.¹⁶

FESEM examinations

The FESEM images of GON show a layered structure as illustrated in Fig. 5a. PANI particles seem to be smaller than 50 nm which are partially agglomerated in some sections. This is shown in Fig. 5b. Different percentages of GON in the PANI-GON nanocomposite in the FESEM images are shown in Fig. 5. By introducing small amounts of graphene oxide into the polyaniline structure via in situ polymerization, the structure of polyaniline has changed. In a low magnification, the holes which are created during the synthesis process are detected. This structure is well known as honey beehive structure.⁴¹ The polyaniline has nanosphere structure and the particle size of the PANI nanocomposite is in the range of 44–48 nm. The structure of the PANI-GON nanocomposites looks like a 1D material. The external diameter of these nanocomposites was measured around 23–40 nm. The layered structure of GON is clearly observed in the PANI-GON (24 wt%) nanocomposite. This inhomogeneous structure will affect the dispersion of PANI-GON (24 wt%) nanocomposite in the epoxy matrix and consequent protective properties as will be discussed.

Corrosion resistance of epoxy/PANI-GON coatings

Electrochemical impedance spectroscopy (EIS) studies

In order to study the corrosion behavior of the nanocomposite coatings, EIS measurements were

taken. Figure 6 illustrates two different equivalent circuit models (ECM) which were used at various immersion times to interpret the EIS plots and hence the corrosion behavior. The parameters introduced here are R_s , R_c , R_{ct} , CPE_c , CPE_{dl} , and W which represent the electrolyte resistance, the coating pore resistance, the charge transfer resistance, the constant phase element of the coating capacitor, double layer capacitance, and Warburg impedance, respectively. The amounts of R_s for all tests were smaller than those of R_c and R_{ct} . The surface of carbon steel substrate was coated using epoxy matrix coatings containing (2 wt%) PANI-GON nanocomposites and immersed in a 3.5% NaCl solution.⁴⁹ Introduction of epoxy in the coating structures prompts the scientists to predict two loops in their equivalent circuits. The common explanation of the impedance diagrams containing two capacitive loops is that the high-frequency section corresponds to the organic coating in which the electric flow consistently is distributed through the coating material. Meanwhile, the reactions taking place in pores and defects can develop in the low-frequency section. At low frequencies, the electric flow through the pores is higher.^{50,51}

EIS evaluations were employed to detect the corrosion performance of neat epoxy, epoxy/PANI, epoxy/PANI-GON (3 wt%), epoxy/PANI-GON (6 wt%), epoxy/PANI-GON (12 wt%), and epoxy/PANI-GON (24 wt%) coatings applied on the carbon steel substrates. Figures 7 and 8 show the Nyquist (a1, b1, c1) and Bode (a2, b2, c2) plots of the samples after immersion in 3.5 wt% NaCl solution for different intervals of time, including 2, 24, 144, and 192 h. The evaluation parameters which were extracted by equivalent circuits are listed in Table 1 for different coatings.

The Z value which is shown by Bode plots at low frequencies ($|Z|_{0.1 \text{ Hz}}$) is determined to define corrosion resistance of the coatings.^{52,53} Generally, the impedance of the samples decreases by increasing immersion time due to the diffused electrolyte into the micropores of the coating. However, at this stage, the electrolyte could not penetrate at the interface of coating/steel in spite of the existence of pores in the coating structure which were not filled with nanocomposites. Besides, a small amount of electrolyte could reach the surface of metal substrate despite the fact that the pores of epoxy were filled with nanocomposite. In this case, the corrosion process can take place at the interface of the coating/steel, and the related products accumulate at the interface of the coating and surface of the metal. After accumulation of corrosion products, the impedance of samples completely changed for some of the coatings with poor resistance. Moreover, the coating resistance values obtained from the EIS test often increase, revealing the fact that the passive layer covers the metal surface which in turn slows down the corrosion reaction and thus protects the surface.⁵⁴ According to Figs. 7 and 8, epoxy/PANI-GON (3 wt%), epoxy/PANI-GON (6 wt%),

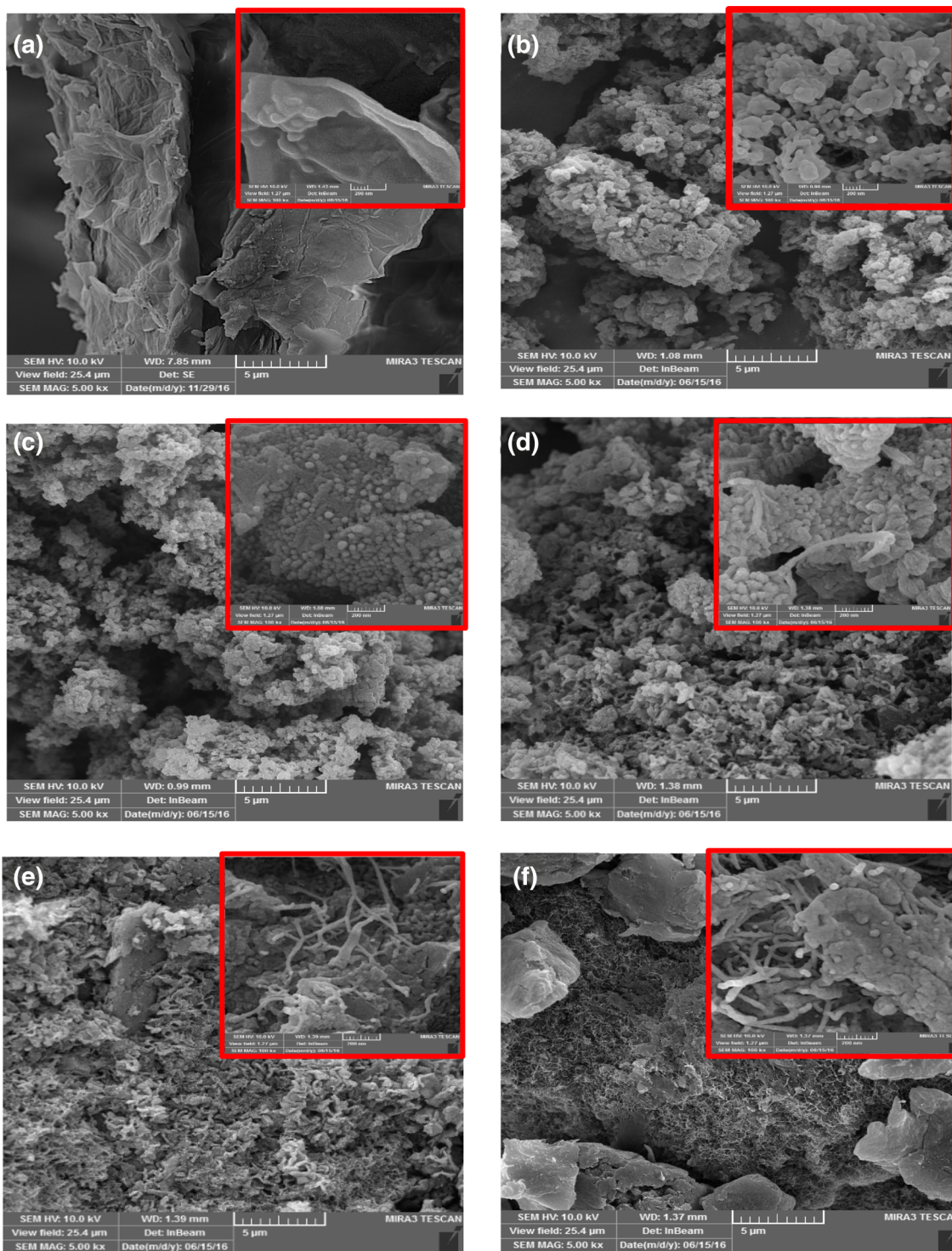


Fig. 5: FESEM images: (a) GON, (b) PANI, (c) PANI-GON (3 wt%), (d) PANI-GON (6 wt%), (e) PANI-GON (12 wt%), (f) PANI-GON (24 wt%)

epoxy/PANI-GON (12 wt%), and epoxy/PANI-GON (24 wt%) nanocomposite coatings have extremely high $|Z|_{0.1\text{Hz}}$ values compared to pure epoxy and epoxy/PANI coatings, showing the high corrosion protection

efficiency of the nanocomposite coatings. Furthermore, $|Z|_{0.1\text{Hz}}$ values of epoxy/PANI-GON (6 wt%) and epoxy/PANI-GON (12 wt%) are remarkably higher than the other mentioned samples. This result shows the

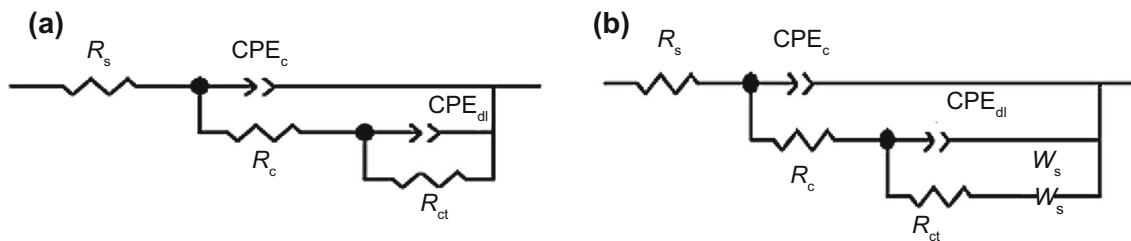


Fig. 6: Equivalent circuits which were proposed for fitting the EIS data

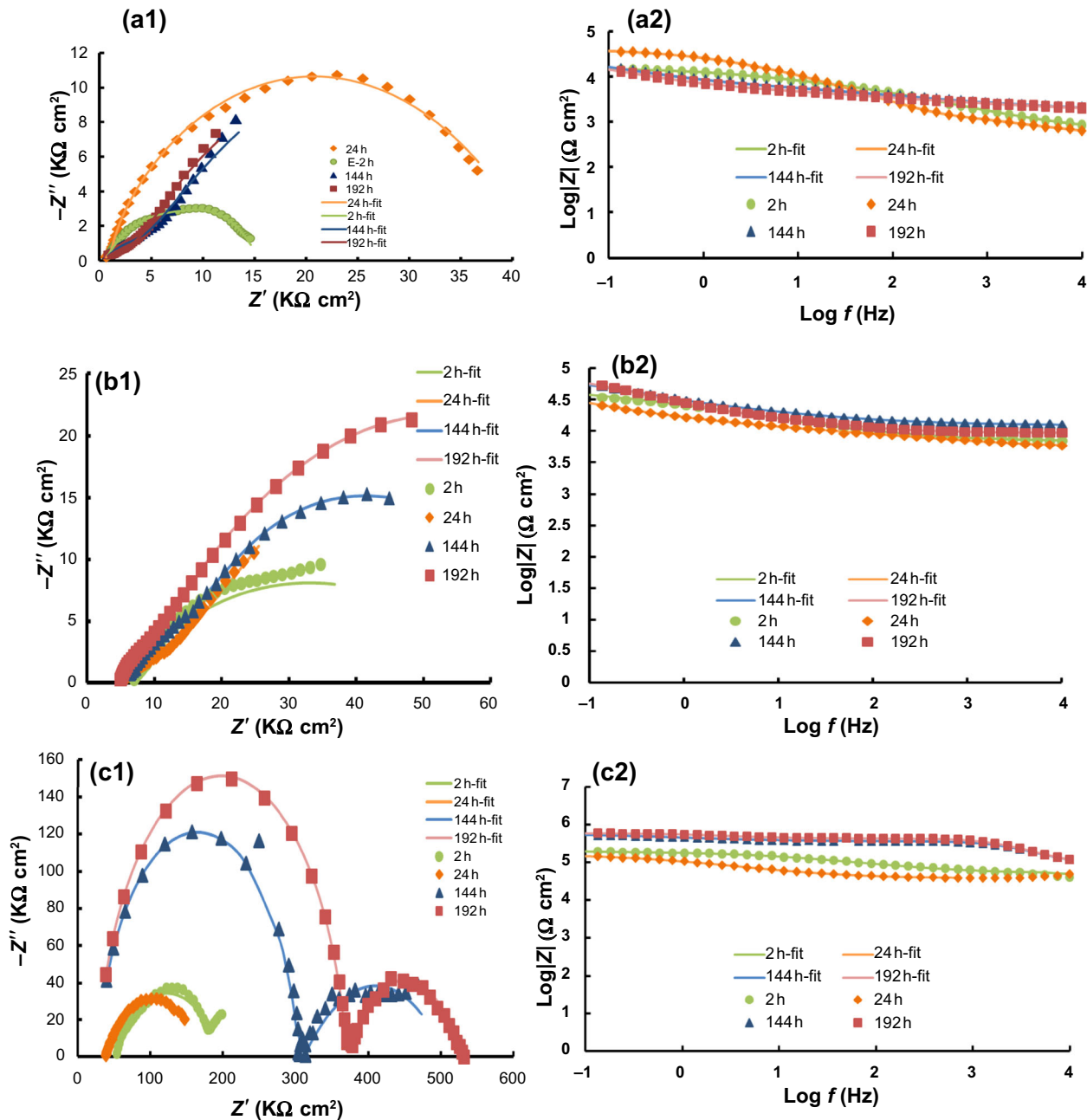


Fig. 7: (a1) Nyquist and (a2) bode plots for epoxy sample; (b1) Nyquist and (b2) bode plots for PANI sample; (c1) Nyquist and (c2) bode plots for epoxy/PANI-GON (3 wt%) sample in the duration of the EIS tests

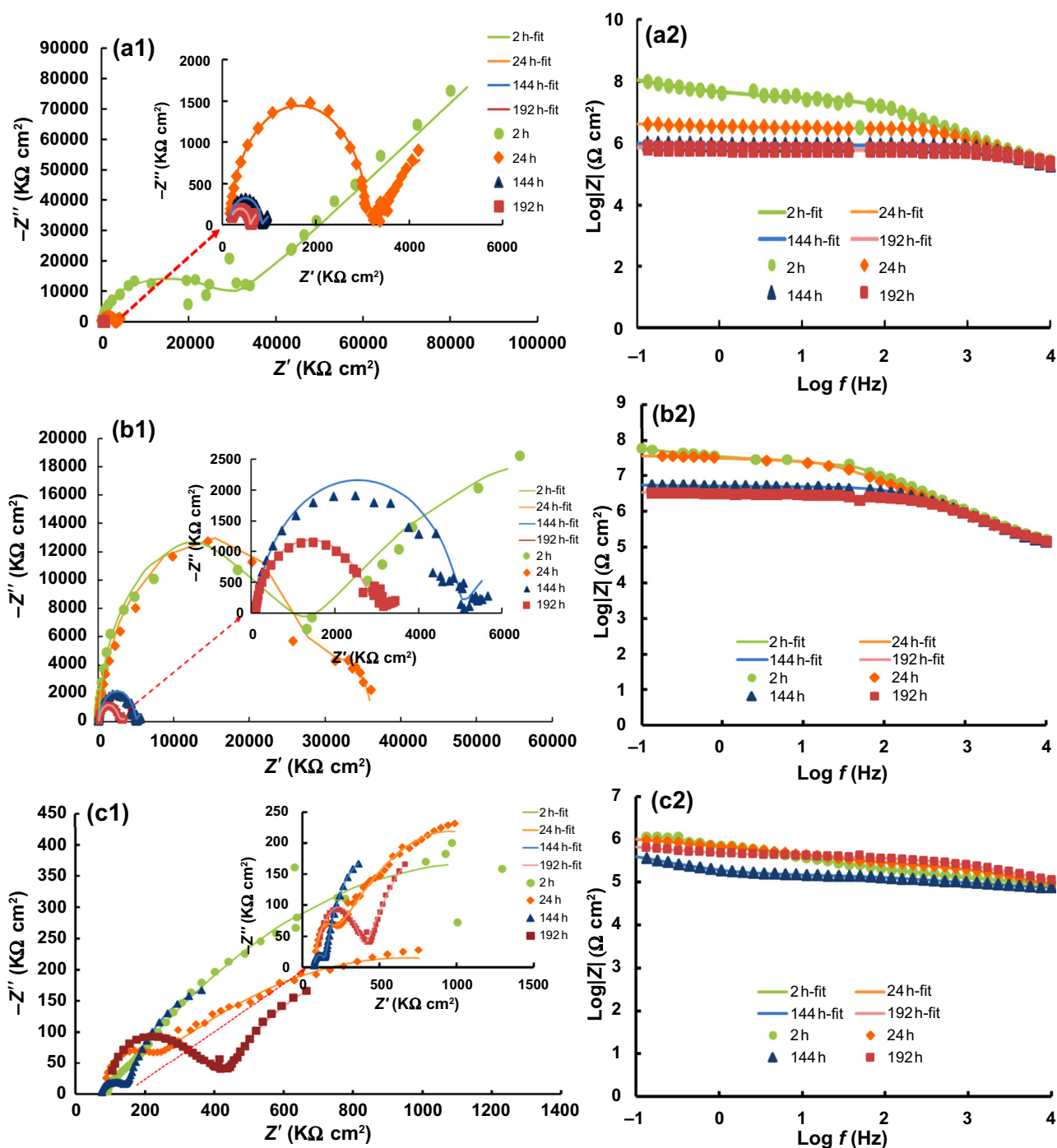


Fig. 8: (a1) Nyquist and (a2) bode plots for epoxy/PANI-GON (6 wt%) sample; (b1) Nyquist and (b2) bode plots for epoxy/PANI-GON (12 wt%) sample; (c1) Nyquist and (c2) bode plots for epoxy/PANI-GON (24 wt%) sample in the duration of the EIS tests

excellent performance of these nanocomposite coatings. The percentage of GON in the PANI-GON nanocomposite has a significant effect on the quality of the coatings. The corrosion resistance of coatings in view of PANI-GON nanofillers increases in the following order: neat epoxy < epoxy/PANI < epoxy/PANI-GON (3 wt%)

< epoxy/PANI-GON (24 wt%) < epoxy/PANI-GON (6 wt%) < epoxy/PANI-GON (12 wt%).

As shown in Figs. 8a1 and 8a2, Warburg impedance appears only after 2 h in epoxy/PANI-GON (6 wt%) coating in low frequency. This likely happened due to the fact that the diffusion of corrosive species may have

Table 1: Electrochemical parameters of different kind of coatings on carbon steel in 3.5 wt% NaCl solution

Time (h)	R_c (Ω cm ²)	CPE_c (nF cm ⁻²)	R_{ct} (Ω cm ²)	CPE_{dl} (nF cm ⁻²)	
Epoxy (E)					
2	1.01×10^4	4.87×10^{-6}	4.73×10^3	2.80×10^{-5}	
24	2.13×10^3	6.87×10^{-6}	4.03×10^4	2.44×10^{-7}	
144	9.90×10^3	3.49×10^{-5}	2.10×10^4	4.81×10^{-5}	
192	1.00×10^4	5.77×10^{-5}	2.49×10^4	5.21×10^{-5}	
PANI					
2	9.29×10^3	6.75×10^{-6}	5.04×10^4	2.11×10^{-5}	
24	1.67×10^4	1.44×10^{-5}	3.83×10^4	3.83×10^{-5}	
144	3.49×10^4	1.34×10^{-5}	3.84×10^4	9.15×10^{-6}	
192	6.82×10^3	2.79×10^{-6}	8.70×10^4	1.63×10^{-5}	
Epoxy/PANI-GON (3 wt%)					
2	1.45×10^5	4.44×10^{-7}	7.25×10^4	6.91×10^{-5}	
24	8.01×10^3	1.36×10^{-7}	1.21×10^5	3.06×10^{-6}	
144	2.73×10^5	2.57×10^{-7}	2.19×10^5	2.06×10^{-6}	
192	3.41×10^5	2.80×10^{-10}	1.67×10^5	7.81×10^{-7}	
Time (h)	R_c (Ω cm ²)	CPE_c (nF cm ⁻²)	R_{ct} (Ω cm ²)	CPE_{dl} (nF cm ⁻²)	W (Ω^{-1} s ⁿ cm ⁻²)
Epoxy/PANI-GON (6 wt%)					
2	2.67×10^7	9.88×10^{-11}	6.00×10^7	1.07×10^{-8}	9.00×10^8
24	2.93×10^6	1.26×10^{-10}	2.25×10^6	7.32×10^{-7}	–
144	6.86×10^5	1.90×10^{-10}	4.38×10^5	6.57×10^{-6}	–
192	4.37×10^5	2.91×10^{-10}	3.80×10^5	7.13×10^{-6}	–
Time (h)	R_c (Ω cm ²)	CPE_c (nF cm ⁻²)	R_{ct} (Ω cm ²)	CPE_{dl} (nF cm ⁻²)	
Epoxy/PANI-GON (12 wt%)					
2	2.40×10^7	1.52×10^{-10}	5.59×10^7	2.45×10^{-8}	
24	2.70×10^7	3.62×10^{-10}	7.01×10^6	4.20×10^{-8}	
144	4.91×10^6	3.18×10^{-10}	9.53×10^5	1.15×10^{-6}	
192	2.70×10^6	2.64×10^{-10}	8.00×10^5	5.10×10^{-7}	
Epoxy/PANI-GON (24 wt%)					
2	2.78×10^5	2.85×10^{-7}	1.86×10^6	3.09×10^{-7}	
24	5.73×10^4	3.50×10^{-7}	1.62×10^6	6.67×10^{-7}	
144	6.36×10^4	1.30×10^{-7}	9.53×10^5	1.15×10^{-6}	
192	3.21×10^5	8.12×10^{-9}	6.11×10^5	3.14×10^{-6}	

been suppressed. It is noteworthy that the results obtained for epoxy/PANI-GON (6 wt%) coating after 2 h can be fitted by equivalence circuit of Fig. 6b. Thus, the high Warburg resistance value demonstrates good capability of the PANI-GON (6 wt%) nanocomposites incorporated into the epoxy matrix for the protection of the metallic substrate in the corrosive environment.^{49,55} Beyond that, the GON percentage in the structure of nanocomposites plays an important role in obtaining promising results for corrosion protection. The barrier properties of coatings against corrosion will be different as a result of exfoliation and dispersion quality of synthesized nanocomposites in the epoxy matrix. Therefore, epoxy/PANI-GON (24 wt%) shows a less protective quality of the surface from corrosion, which is related to the poor dispersion ability of PANI-GON (24 wt%) in filling the epoxy micropores. We understand that the corrosion protection of our developed nanocomposite coatings was realized by different methods. First, the protection can

be achieved by filling the micropores of the epoxy matrix and also by changing the direction and the length of the transport paths of corrosive species to the surface. In fact, the paths are changed from straight to zigzag paths which are longer. The PANI-GON nanocomposites in the epoxy matrix limit the electrolyte diffusion and could restrict the electrolyte paths, thereby increasing the diffusion length. Second, protection can be achieved by creating active coatings on the surface of the metal. Moreover, the PANI-GON nanocomposite could resist against Cl⁻ ions diffusion as a result of the negative surface charge of PANI-GON in the epoxy matrix.^{56,57}

Capacitance and resistance of coatings

Figure 9 depicts the variation of coating resistance as a function of immersion time in 3.5 wt% NaCl solution. In principle, epoxy/PANI-GON (6 wt%) and epoxy/

PANI-GON (12 wt%) coatings are more corrosion resistant than the other coatings and have significantly different corrosion resistance with other coatings. A possible reason for this observation could be due to a well-dispersed PANI-GON nanocomposites in the epoxy matrix. In contrast, for other nanocomposites, in particular PANI-GON (24 wt%) there is a huge difference in the coating resistance with other composite loadings as seen in Fig. 9 which may be described by its low dispersion capabilities. However, we observed two different time-dependent corrosion behaviors. (1) For the coatings with relatively higher resistance, mentioned above, the coating resistance gradually decreases which might be attributed to the presence of graphene oxide in structures of the nanocomposites making them more hydrophobic due to oxygen groups on the surface of graphene sheets.³⁶ (2) For low resistance coatings such as epoxy, epoxy/PANI, epoxy/PANI-GON (3 wt%), and epoxy/PANI-GON (24 wt%), after an initial decrease, the corrosion resistance of the coatings increases as a function of immersion time. This increase can be ascribed to the formation of a passive layer produced by diffusion of the electrolyte into the interface of the coating through the pores and defects toward the steel substrate surface. Passive layer can protect the surface from further corrosion elements and keep the water away from reaching the surface of the metal.

The coating capacitance is an appropriate quantity to measure electrolyte permeation into the coating structure. The electrolyte diffusion can affect the dielectric constant of coating which is here defined as a constant phase element CPE_c . The variation of CPE_c obtained after different immersion times is listed in Table 1. CPE_c values for the pure epoxy coating increase gradually during the immersion time. This indicates that the diffusion process could be performed easily and that the epoxy coating would lose its protection performance very quickly. Penetration of

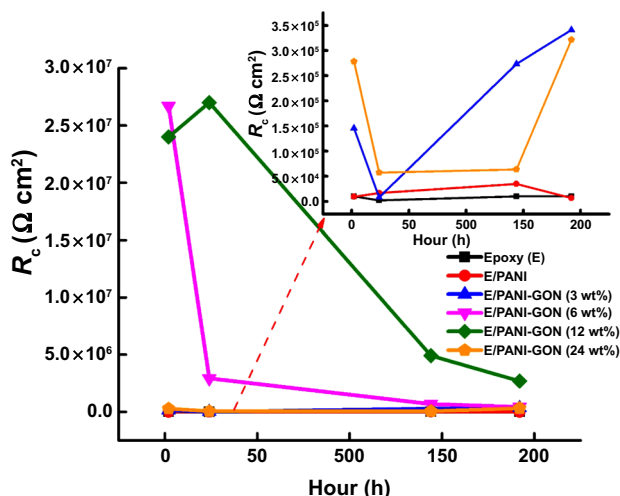


Fig. 9: The distinction of the R_c for the six coatings

the aqueous electrolyte into the coating can cause some problems including swelling of the coating and blistering at some thin or defect parts. This can form direct paths for corrosion species to get access onto the metal substrate. In addition, the CPE_c values obtained for the epoxy/PANI-GON (6 wt%) and epoxy/PANI-GON (12 wt%) are lower than for other coatings. The lowest CPE_c value for epoxy/PANI-GON (6 wt%) coating was obtained after 2 h immersion. The reason for this was explained by introducing Warburg element in the equivalent electrical circuit shown previously in Fig. 6b which was fitted to the experimental EIS data and reported in Table 1.

For longer immersion time in the saline water, the values of CPE_c for epoxy/PANI-GON (6 wt%) and epoxy/PANI-GON (12 wt%) increase over time; therefore, the resistance of the coatings decreased. Increasing the amount of CPE_c for the epoxy/PANI-GON (12 wt%) was faster than for epoxy/PANI-GON (6 wt%) which indicates that Warburg impedance was neglected. These results reported in Table 1 exhibit that the PANI-GON (6 wt%) and PANI-GON (12 wt%) nanocomposites could reduce the number of diffusion paths from the electrolyte toward the substrate surface. For other coatings studied, we observed an increase of CPE_c values over time indicating that the electrolyte has reached the surface of the metal. Any further decrease in CPE_c implies that a passive layer may form at the interface of the coating/metal substrate. This will block further diffusion paths by filling the possible micropores in the coating, thereby preventing the entrance of corrosive elements into the coating structure. However, in some cases subsequent increase of CPE_c might be due to probable destruction of the passive layer formed initially. Based on the argument given above as well as the magnitudes of other effective parameters like R_{ct} , the charge transfer resistance and CPE_{dl} , double-layer capacitance which are summarized in Table 1, we understand that epoxy/PANI-GON (12 wt%) is the most corrosion resistant coating among all types of coatings studied here. The epoxy/PANI-GON (12 wt%) coating did exhibit satisfactory wet adhesion force as shown in Table 1. The lowest value of the CPE_{dl} is observed for epoxy/PANI-GON (12 wt%) coating at the end of 192-h immersion.

Demonstration of the anticorrosion function of epoxy/PANI-GON nanocomposite coatings

Figure 10 schematically represents the function of PANI-GON nanocomposite in the epoxy matrix for protecting the metallic surface from corrosive environment. In panel (a), the pure epoxy coating on metal is shown in which the micropores are not filled with nanocomposite, and coating is colorless. Therefore, the electrolyte may readily diffuse to the interface of the coating/steel. In panel (b), the micropores of the epoxy coating were filled with nanocomposites, and the color

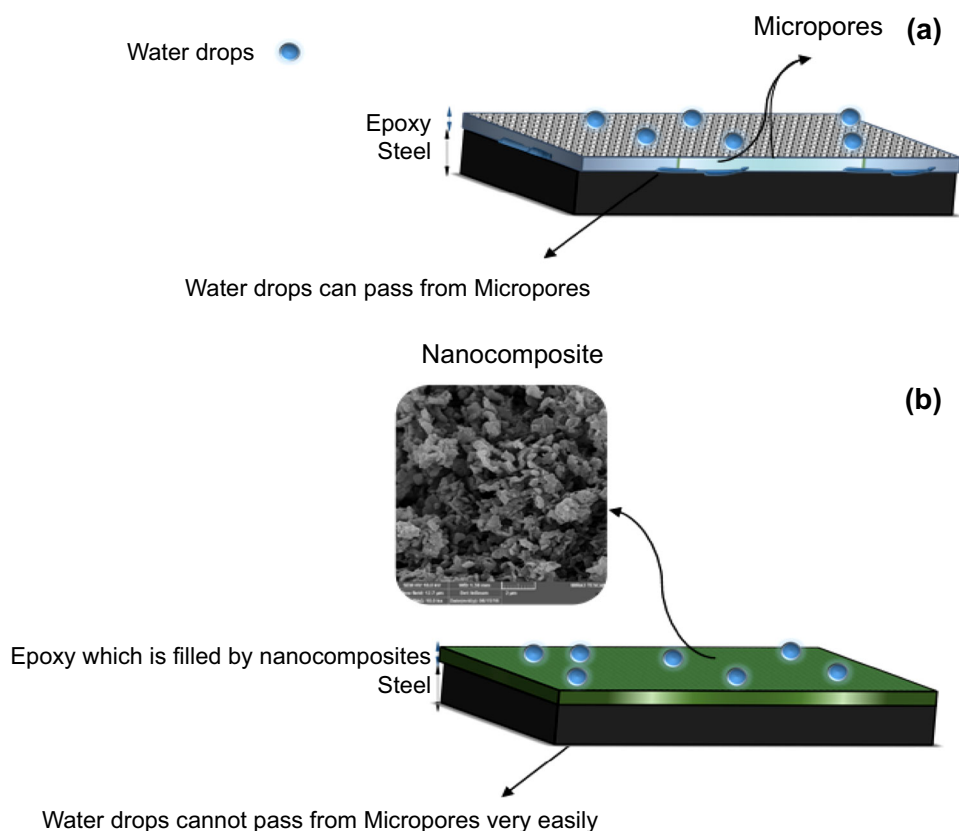


Fig. 10: Schematic of epoxy/PANI-GON coatings function in the duration of contact with electrolyte

of the coating turned green. Moreover, this schematic picture illustrates that the introduction of the prepared nanocomposites with complex structure into the epoxy matrix can restrict the diffusion process of electrolyte droplets and prevent them from reaching the surface of the metal by creating zigzag paths (longer paths) for diffusion via the entrance of the mentioned nanocomposites within the micropores.

Antifouling properties of epoxy/PANI-GON coatings

Antifouling properties of coating samples were carried out by immersing them in the test cell comprising of spirulina algae, guppy fish, and dwarf hair grass for three months. After three months, the coated samples were washed and dried. A reference sample (epoxy coating sample) was used to compare the antifouling performance of immersed coatings. Figure 11 shows that the sample with pure epoxy coating had poor antifouling quality; therefore the fouling process seems to be more intense at the interface of the metal and coating easily. The formation of a new green layer clearly confirms the fouling which is shown in Fig. 11. According to the results, epoxy/PANI-GON (6 wt%) and epoxy/PANI-GON (12 wt%) coatings exhibit higher antifouling capability than other coatings. The

quality of epoxy/PANI-GON (24 wt%) coating is rather poor. The paint coating almost disintegrated from the interface of the steel substrate.

Conclusion

An in situ polymerization method was used for the synthesis of PANI-GON nanocomposites. These nanocomposites were analyzed by different methods including FESEM, FTIR, and XRD. The prepared nanocomposites were added into the epoxy matrix making epoxy/PANI-GON paint coating to improve the inherent quality of epoxy in terms of the anticorrosion and antifouling properties. EIS investigations reveal that epoxy/PANI-GON coatings have higher resistance against corrosive environment than epoxy and/or epoxy/PANI coatings. The amount of graphene oxide in the structure of nanocomposites can affect the dispersion ability of the nanocomposite in the epoxy matrix and thereby the function of the coatings in the corrosive environment. For epoxy/PANI-GON (6 wt%) and epoxy/PANI-GON (12 wt%) coatings, good dispersion of GON in PANI and subsequently in epoxy was achieved which leads to higher corrosion resistance. At higher GON ratio, for instance epoxy/PANI-GON (24 wt%) graphene oxide showed less ability to disperse and fill the micropores of the epoxy,

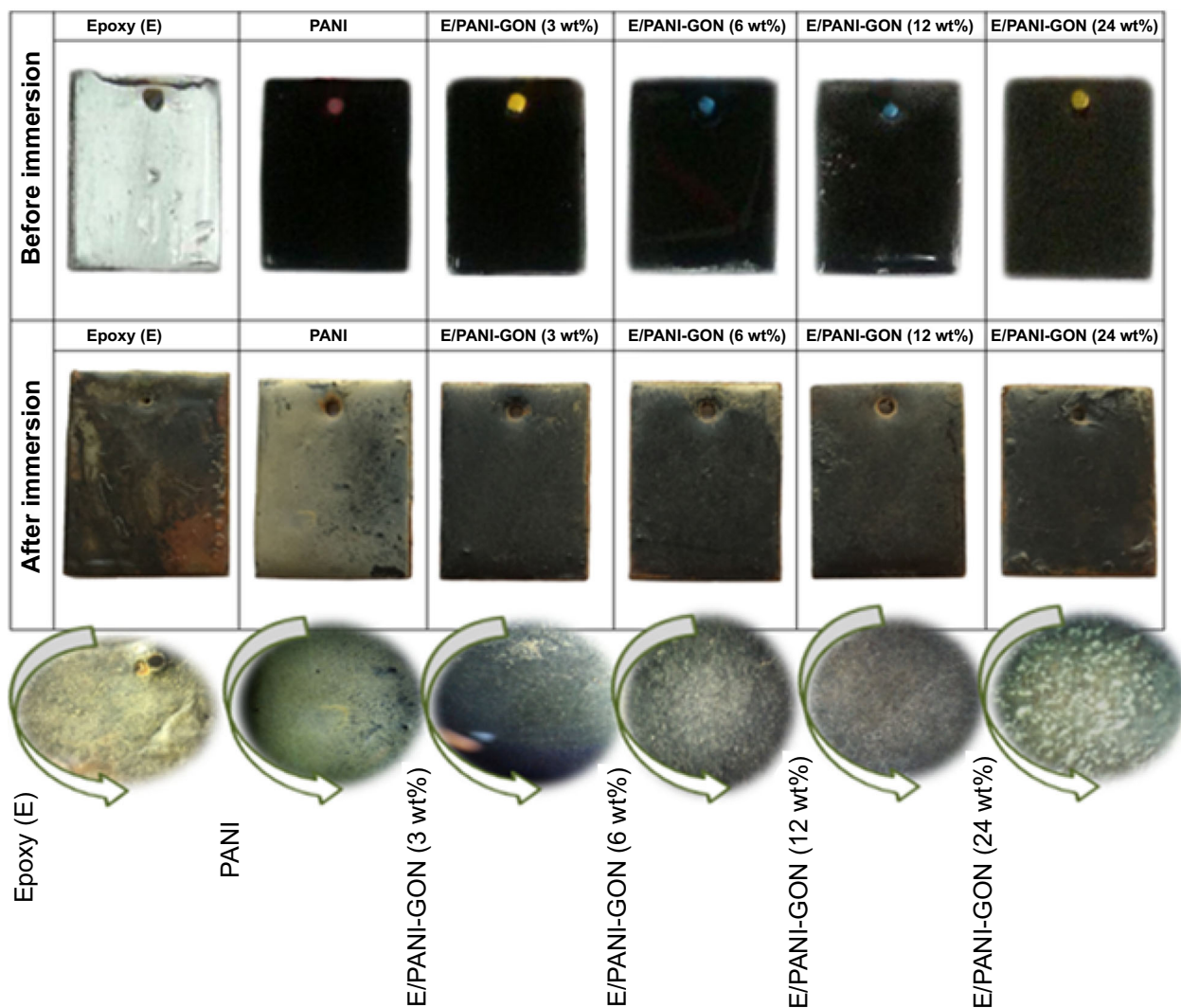


Fig. 11: Coating samples before and after immersion in aquarium for 3 month

and the obtained composite shows lower resistance against corrosive elements. In comparison between EIS values of epoxy coatings with and without nanocomposite filling, we find that coating resistance (R_c) value of epoxy/PANI-GON (12 wt%) was 2.70×10^6 which is 7.9 times higher than epoxy/PANI-GON (3 wt%) after 192-h immersion in the 3.5 wt% NaCl solution. The highest resistance values detected by EIS tests in saline water are those for the epoxy/PANI-GON (12 wt%) coating. The antifouling property of the coatings was investigated in a simulated environment. After 3 months of immersion in simulated sea water containing microorganisms, the epoxy and epoxy/PANI coatings and epoxy/PANI-GON (6 and 12 wt%) showed the lowest and the highest antifouling behavior, respectively. The reason could be the incorporation of PANI-GON nanocomposites into epoxy to fill the micropores. Further detailed studies need to prove mechanistic information on the antifouling behavior of the coatings.

Acknowledgments The authors would like to thank the Sahand University of Technology of Tabriz and University of Tabriz and Iranian Nanotechnology Initiative Council for the financial support of this project.

References

1. Koch, GH, Brongers, MP, Thompson, NG, Virmani, YP, Payer, JH, "Corrosion Cost and Preventive Strategies in the United States." (2002)
2. Ramón, JE, Gandía-Romero, JM, Valcuende, M, Bataller, R, "Integrated Sensor Network for Monitoring Steel Corrosion in Concrete Structures." *VITRUVIO-Int. J. Archit. Technol. Sustain.*, **1** (1) 65–79 (2016)
3. Böhm, S, "Graphene Against Corrosion." *Nat. Nanotechnol.*, **9** (10) 741–742 (2014)

4. Rathish, RJ, Dorothy, R, Joany, R, Pandiarajan, M, “Corrosion Resistance of Nanoparticle-Incorporated Nano Coatings.” *Eur. Chem. Bull.*, **2** (12) 965–970 (2013)
5. Zvonkina, I, Soucek, M, “Inorganic–Organic Hybrid Coatings: Common and New Approaches.” *Curr. Opin. Chem. Eng.*, **11** 123–127 (2016)
6. Montemor, M, “Functional and Smart Coatings for Corrosion Protection: A Review of Recent Advances.” *Surf. Coat. Technol.*, **258** 17–37 (2014)
7. Nine, MJ, Cole, MA, Tran, DN, Losic, D, “Graphene: A Multipurpose Material for Protective Coatings.” *J. Mater. Chem. A*, **3** (24) 12580–12602 (2015)
8. Hellio, C, Yebra, D, *Advances in Marine Antifouling Coatings and Technologies*. Elsevier, Amsterdam, 2009
9. Nurioglu, AG, Esteves, ACC, “Non-Toxic, Non-Biocide-Release Antifouling Coatings Based on Molecular Structure Design for Marine Applications.” *J. Mater. Chem. B*, **3** (32) 6547–6570 (2015)
10. Sørensen, PA, Kiil, S, Dam-Johansen, K, Weinell, CE, “Anticorrosive Coatings: A Review.” *J. Coat. Technol. Res.*, **6** (2) 135–176 (2009)
11. Novoselov, KS, Geim, AK, Morozov, SV, Jiang, D, Zhang, Y, Dubonos, SV, Grigorieva, IV, Firsov, AA, “Electric Field Effect in Atomically Thin Carbon Films.” *Science*, **306** (5696) 666–669 (2004)
12. Martin-Gallego, M, Verdejo, R, Lopez-Manchado, M, Sangermano, M, “Epoxy-Graphene UV-Cured Nanocomposites.” *Polymer*, **52** (21) 4664–4669 (2011)
13. Wang, H, Hao, Q, Yang, X, Lu, L, Wang, X, “Effect of Graphene Oxide on the Properties of its Composite with Polyaniline.” *ACS Appl. Mater. Interfaces*, **2** (3) 821–828 (2010)
14. Zhang, WL, Liu, YD, Choi, HJ, “Fabrication of Semiconducting Graphene Oxide/Polyaniline Composite Particles and their Electrorheological Response Under an Applied Electric Field.” *Carbon*, **50** (1) 290–296 (2012)
15. Nasrollahzadeh, M, Babaei, F, Fakhri, P, Jaleh, B, “Synthesis, Characterization, Structural, Optical Properties and Catalytic Activity of Reduced Graphene Oxide/Copper Nanocomposites.” *RSC Adv.*, **5** (14) 10782–10789 (2015)
16. Huang, Y, Lin, C, “Polyaniline-Intercalated Graphene Oxide Sheet and its Transition to a Nanotube Through a Self-curling Process.” *Polymer*, **53** (5) 1079–1085 (2012)
17. Huang, X, Qi, X, Boey, F, Zhang, H, “Graphene-Based Composites.” *Chemical Society Reviews*, **41** (2) 666–686 (2012)
18. Zhu, Y, Murali, S, Cai, W, Li, X, Suk, JW, Potts, JR, Ruoff, RS, “Graphene and Graphene Oxide: Synthesis, Properties, and Applications.” *Advanced Materials*, **22** (35) 3906–3924 (2010)
19. Pumera, M, “Electrochemistry of Graphene: New Horizons for Sensing and Energy Storage.” *The Chemical Record*, **9** (4) 211–223 (2009)
20. Wei, J, Vo, T, Inam, F, “Epoxy/Graphene Nanocomposites—Processing and Properties: A Review.” *RSC Advances*, **5** (90) 73510–73524 (2015)
21. Shi, X, Nguyen, TA, Suo, Z, Liu, Y, Avci, R, “Effect of Nanoparticles on the Anticorrosion and Mechanical Properties of Epoxy Coating.” *Surface and Coatings Technology*, **204** (3) 237–245 (2009)
22. Dominis, AJ, Spinks, GM, Wallace, GG, “Comparison of Polyaniline Primers Prepared with Different Dopants for Corrosion Protection of Steel.” *Prog. Org. Coat.*, **48** (1) 43–49 (2003)
23. Fang, J, Xu, K, Zhu, L, Zhou, Z, Tang, H, “A Study on Mechanism of Corrosion Protection of Polyaniline Coating and its Failure.” *Corros. Sci.*, **49** (11) 4232–4242 (2007)
24. Schauer, T, Joos, A, Dulog, L, Eisenbach, C, “Protection of Iron Against Corrosion with Polyaniline Primers.” *Prog. Org. Coat.*, **33** (1) 20–27 (1998)
25. Hartwig, A, Sebald, M, Pütz, D, Aberle, L, “Preparation, Characterisation and Properties of Nanocomposites Based on Epoxy Resins—An Overview.” *Proc. Macromolecular Symposia* (2005)
26. Becker, O, Varley, R, Simon, G, “Morphology, Thermal Relaxations and Mechanical Properties of Layered Silicate Nanocomposites Based upon High-Functionality Epoxy Resins.” *Polymer*, **43** (16) 4365–4373 (2002)
27. Yang, L, Liu, F, Han, E, “Effects of P/B on the Properties of Anticorrosive Coatings with Different Particle Size.” *Prog. Org. Coat.*, **53** (2) 91–98 (2005)
28. Lamaka, SV, Zheludkevich, ML, Yasakau, KA, Serra, R, Poznyak, S, Ferreira, M, “Nanoporous Titania Interlayer as Reservoir of Corrosion Inhibitors for Coatings with Self-healing Ability.” *Prog. Org. Coat.*, **58** (2) 127–135 (2007)
29. Shi, H, Liu, F, Yang, L, Han, E, “Characterization of Protective Performance of Epoxy Reinforced with Nanometer-Sized TiO₂ and SiO₂.” *Prog. Org. Coat.*, **62** (4) 359–368 (2008)
30. Pourhashem, S, Vaezi, MR, Rashidi, A, “Investigating the Effect of SiO₂-Graphene Oxide Hybrid as Inorganic Nanofiller on Corrosion Protection Properties of Epoxy Coatings.” *Surf. Coat. Technol.*, **311** 282–294 (2017)
31. Yu, Z, Di, H, Ma, Y, He, Y, Liang, L, Lv, L, Ran, X, Pan, Y, Luo, Z, “Preparation of Graphene Oxide Modified by Titanium Dioxide to Enhance the Anti-Corrosion Performance of Epoxy Coatings.” *Surf. Coat. Technol.*, **276** 471–478 (2015)
32. Mostafaei, A, Nasirpour, F, “Electrochemical Study of Epoxy Coating Containing Novel Conducting Nanocomposite Comprising Polyaniline–ZnO Nanorods on Low Carbon Steel.” *J. Coat. Technol. Res.*, **10** (5) 679–694 (2013)
33. Mostafaei, A, Nasirpour, F, “Preparation and Characterization of a Novel Conducting Nanocomposite Blended with Epoxy Coating for Antifouling and Antibacterial Applications.” *Corros. Eng. Sci. Technol.*, **48** (7) 513–524 (2014)
34. Mostafaei, A, Nasirpour, F, “Epoxy/Polyaniline–ZnO Nanorods Hybrid Nanocomposite Coatings: Synthesis, Characterization and Corrosion Protection Performance of Conducting Paints.” *Prog. Org. Coat.*, **77** (1) 146–159 (2014)
35. Jafari, Y, Ghoreishi, SM, Shabani-Nooshabadi, M, “Electrochemical Deposition and Characterization of Polyaniline–Graphene Nanocomposite Films and its Corrosion Protection Properties.” *J. Polym. Res.*, **23** (5) 91 (2016)
36. Mooss, VA, Bhopale, AA, Deshpande, PP, Athawale, AA, “Graphene Oxide-Modified Polyaniline Pigment for Epoxy Based Anti-Corrosion Coatings.” *Chem. Pap.*, **71** (8) 1515–1528 (2017)
37. Zhang, K, Zhang, LL, Zhao, X, Wu, J, “Graphene/Polyaniline Nanofiber Composites as supercapacitor Electrodes.” *Chem. Mater.*, **22** (4) 1392–1401 (2010)
38. Nasirpour, F, Pourmahmoudi, H, Abbasi, F, Littlejohn, S, Chauhan, AS, Nogaret, A, “Modification of Chemically Exfoliated Graphene to Produce Efficient Piezoresistive Polystyrene-Graphene Composites.” *J. Electron. Mater.*, **44** (10) 3512 (2015)
39. Huang, Y, Lin, C, “Facile Synthesis and Morphology Control of Graphene Oxide/Polyaniline Nanocomposites Via In Situ Polymerization Process.” *Polymer*, **53** (13) 2574–2582 (2012)
40. Yin, Q, Shu, R, Xing, H, Tan, D, Gan, Y, Xu, G, “Rheological Behavior and Electrical Properties of Graphene Oxide/Polyaniline Nanocomposites.” *Nano*, **11** (02) 1650020 (2016)

41. Li, M, Yin, W, Han, X, Chang, X, “Hierarchical Nanocomposites of Polyaniline Scales Coated on Graphene Oxide Sheets for Enhanced Supercapacitors.” *J. Solid State Electrochem.*, **20** (7) 1941–1948 (2016)
42. Thema, F, Moloto, M, Dikio, E, Nyangiwe, N, Kotsedi, L, Maaza, M, Khenfouch, M, “Synthesis and Characterization of Graphene Thin Films by Chemical Reduction of Exfoliated and Intercalated Graphite Oxide.” *J. Chem.*, **2013** (2012)
43. Sun, J, Bi, H, “Pickering Emulsion Fabrication and Enhanced Supercapacity of Graphene Oxide-Covered Polyaniline Nanoparticles.” *Mater. Lett.*, **81** 48–51 (2012)
44. Shunaev, VV, Glukhova, OE, “Topology Influence on the Process of Graphene Functionalization by Epoxy and Hydroxyl Groups.” *J. Phys. Chem. C*, **120** (7) 4145–4149 (2016)
45. Wei, H, Zhu, J, Wu, S, Wei, S, Guo, Z, “Electrochromic Polyaniline/Graphite Oxide Nanocomposites with Endured Electrochemical Energy Storage.” *Polymer*, **54** (7) 1820–1831 (2013)
46. Hu, F, Li, W, Zhang, J, Meng, W, “Effect of Graphene Oxide as a Dopant on the Electrochemical Performance of Graphene Oxide/Polyaniline Composite.” *J. Mater. Sci. Technol.*, **30** (4) 321–327 (2014)
47. Marcano, DC, Kosynkin, DV, Berlin, JM, Sinitskii, A, Sun, Z, Slesarev, A, Alemany, LB, Lu, W, Tour, JM, “Improved Synthesis of Graphene Oxide.” *ACS Nano*, **4** (8) 4806–4814 (2010)
48. Imran, SM, Kim, Y, Shao, GN, Hussain, M, Choa, Y, Kim, HT, “Enhancement of Electroconductivity of Polyaniline/Graphene Oxide Nanocomposites Through In Situ Emulsion Polymerization.” *J. Mater. Sci.*, **49** (3) 1328–1335 (2014)
49. Mohammadi, S, Taromi, FA, Shariatpanahi, H, Neshati, J, Hemmati, M, “Electrochemical and Anticorrosion Behavior of Functionalized Graphite Nanoplatelets Epoxy Coating.” *J. Ind. Eng. Chem.*, **20** (6) 4124–4139 (2014)
50. Liu, C, Bi, Q, Leyland, A, Matthews, A, “An Electrochemical Impedance Spectroscopy Study of the Corrosion Behaviour of PVD Coated Steels in 0.5 N NaCl Aqueous Solution: Part II.: EIS Interpretation of Corrosion Behaviour.” *Corros. Sci.*, **45** (6) 1257–1273 (2003)
51. Hang, TTX, Truc, TA, Nam, TH, Oanh, VK, Jorcín, J-B, Pébère, N, “Corrosion Protection of Carbon Steel by an Epoxy Resin Containing Organically Modified Clay.” *Surf. Coat. Technol.*, **201** (16) 7408–7415 (2007)
52. Pourhashem, S, Rashidi, A, Vaezi, MR, Bagherzadeh, MR, “Excellent Corrosion Protection Performance of Epoxy Composite Coatings Filled with Amino-Silane Functionalized Graphene Oxide.” *Surf. Coat. Technol.*, **317** 1–9 (2017)
53. Sun, W, Wang, L, Wu, T, Wang, M, Yang, Z, Pan, Y, Liu, G, “Inhibiting the Corrosion-Promotion Activity of Graphene.” *Chem. Mater.*, **27** (7) 2367–2373 (2015)
54. Di, H, Yu, Z, Ma, Y, Zhang, C, Li, F, Lv, L, Pan, Y, Shi, H, He, Y, “Corrosion-Resistant Hybrid Coatings Based on Graphene Oxide–Zirconia Dioxide/Epoxy System.” *J. Taiwan Inst. Chem. Eng.*, **67** 511–520 (2016)
55. Mohammadi, S, Shariatpanahi, H, Taromi, FA, Neshati, J, “Electrochemical and Anticorrosion Behaviors of Hybrid Functionalized Graphite Nano-Platelets/Tripolyphosphate in Epoxy-Coated Carbon Steel.” *Mater. Res. Bull.*, **80** 7–22 (2016)
56. Li, M, Ji, X, Cui, L, Liu, J, “In Situ Preparation of Graphene/Polypyrrole Nanocomposite Via Electrochemical Co-Deposition Methodology for Anti-Corrosion Application.” *J. Mater. Sci.*, **52** (20) 12251–12265 (2017)
57. Ramezanzadeh, B, Haeri, Z, Ramezanzadeh, M, “A Facile Route of Making Silica Nanoparticles-Covered Graphene Oxide Nanohybrids (SiO₂-GO); Fabrication of SiO₂-GO/Epoxy Composite Coating with Superior Barrier and Corrosion Protection Performance.” *Chem. Eng. J.*, **303** 511–528 (2016)